

Shortcut to Self-Consistent Light-Matter Interaction and Realistic Spectra from First Principles

Christian Schäfer^{1,2,*} and Göran Johansson^{1,2}

¹*Department of Microtechnology and Nanoscience, MC2, Chalmers University of Technology, 412 96 Göteborg, Sweden*

²*Department of Physics, Chalmers University of Technology, 412 96 Göteborg, Sweden*



(Received 24 September 2021; revised 27 October 2021; accepted 23 March 2022; published 12 April 2022)

We introduce a simple approach to how an electromagnetic environment can be efficiently embedded into state-of-the-art electronic structure methods, taking the form of radiation-reaction forces. We demonstrate that this self-consistently provides access to radiative emission, natural linewidth, Lamb shifts, strong coupling, electromagnetically induced transparency, Purcell-enhanced and superradiant emission. As an example, we illustrate its seamless integration into time-dependent density-functional theory with virtually no additional cost, presenting a convenient shortcut to light-matter interactions.

DOI: [10.1103/PhysRevLett.128.156402](https://doi.org/10.1103/PhysRevLett.128.156402)

The theoretical description of light interacting with realistic materials becomes increasingly interdisciplinary due to the recent developments in nonequilibrium phase transitions [1–3], Floquet engineering [4–6], high-harmonic generation [7,8], strong light-matter coupling and induced modifications of energy transfer [9–18], polaritonic chemistry [19–25], plasmonic strong coupling [26–33], *ab initio* QED [34–39], and quantum-electrodynamical density-functional theory (QEDFT) [39–42]. It is apparent that all light-matter interactions arise from the interplay of matter with a electromagnetic environment. The involved material is routinely described using *ab initio* electronic structure theory. A notable representative is time-dependent density-functional theory (TDDFT) [43,44] due to its good accuracy and comparably low computational cost. While it is common to consider the electromagnetic field as input to the system, i.e., a laser driving the system, the interaction should be treated self-consistently within the *ab initio* calculation according to Maxwell’s equations. This avoids negative side effects such as artificial heating but as we will show here, also naturally introduces a plethora of phenomena such as natural linewidth, Lamb shift, Purcell enhancement [45], superradiance [46,47], strong light-matter coupling and electromagnetically induced transparency [48]. These are common objectives for quantum optics [49] and open quantum-system dynamics but are rarely even considered in state-of-the-art *ab initio* calculations. Existing open-system extensions of density-functional theory [50] are thus far limited in their applicability due to physically less

motivated [51] or much more involved constructions [41,52,53]. The TDDFT codes Salmon [54] and Octopus [53,55] allow the self-consistent propagation of Maxwell and Kohn-Sham equations but the complexity of the implementation and its computational cost limit their widespread use. Only recent developments along the lines of mixed quantum-classical techniques [56], dissipative equations of motion [57], and Casida QEDFT [58] started to address natural lifetimes from first principles. We demonstrate in the following a computationally and conceptually simpler way to extend *ab initio* electronic structure approaches with electromagnetic emission, taking the form of radiation-reaction forces. By embedding Maxwell’s equation of motion into the ordinary TDDFT routine via a simple local potential, we obtain access to open quantum-system dynamics from first principles with virtually no additional effort. Its precise strength is that it allows the description of the aforementioned physical effects without the need to change the existing libraries.

Embedding the electromagnetic environment.— The nonrelativistic dynamic of matter subject to a classical electromagnetic environment is governed by the minimally coupled Coulomb Hamiltonian $\hat{H} = \sum_i [1/(2m_i)] [-i\hbar\nabla_i - q_i\mathbf{A}(\mathbf{r}_i, t)/c]^2 + \hat{H}_{\parallel} + \epsilon_0/2 \int d\mathbf{r} [\mathbf{E}_{\perp}(\mathbf{r}, t)^2 + c^2\mathbf{B}(\mathbf{r}, t)^2]$ with fixed Coulomb gauge $\nabla \cdot \mathbf{A} = 0$. The electromagnetic fields obey Maxwell’s equation of motion and couple self-consistently with the Schrödinger equation. The internal structure of the latter, consisting out of electrons and nuclei, is determined by the longitudinal Coulombic interactions $\hat{H}_{\parallel} = 1/(8\pi\epsilon_0) \sum_{i,j}^{N_e+N_n} q_i q_j / |\mathbf{r}_i - \mathbf{r}_j|$, here given in free-space. The transverse electric $\mathbf{E}_{\perp}(\mathbf{r}, t) = -1/c\partial_t\mathbf{A}(\mathbf{r}, t)$ and magnetic fields $\mathbf{B}(\mathbf{r}, t) = 1/c\nabla \times \mathbf{A}(\mathbf{r}, t)$ are in contrast not bound to the material but can propagate into free-space. Even with the restriction to classical electromagnetic fields we will obtain access to the various

Published by the American Physical Society under the terms of the [Creative Commons Attribution 4.0 International license](https://creativecommons.org/licenses/by/4.0/). Further distribution of this work must maintain attribution to the author(s) and the published article’s title, journal citation, and DOI. Funded by [Bibsam](https://www.bibsam.com/).

highlighted quantum optical effects, while, for instance, the photon blockade [59] will demand quantized fields. If the wavelength of those propagating fields is substantially larger than the matter system, the spatial dependence of the transverse fields is commonly neglected (dipole approximation). Even in this strongly simplified limit, the remaining task of solving the Schrödinger equation is extraordinarily challenging. We will fix the nuclei in the following for brevity but would like to emphasize that their contribution can be easily reinstated by using the total (electronic plus nuclear) dipole. Nuclear motion itself is evidently often a relevant feature to recover experimental spectra.

After performing the Power-Zienau-Wooley transformation [60,61] (see Supplemental Material I [62]), the classical transverse light-matter coupling acting on the electronic structure takes the bilinear form $\hat{V}(t) = -\hat{\mathbf{R}} \cdot \mathbf{E}_\perp(t)$ with the electronic dipole $\hat{\mathbf{R}} = -e \sum_i^{N_e} \mathbf{r}_i$. The electric field can be separated into driving fields $\mathbf{E}_{\text{drive},\perp}$ of external origin and radiated fields $\mathbf{E}_{r,\perp}$ that are generated by the material itself. Naturally, driving the system externally will lead to absorption, excitation, and heat. In principle, we could solve the Schrödinger and Maxwell equations now side by side in order to obtain access to the radiated fields and with it to the self-consistent evolution of light and matter. Given that electrons and fields move at different speeds and scales, this introduces, however, an unnecessary complexity that can be circumvented by the following shortcut.

Each current induces an electromagnetic field for which its precise spatial and polarization structure depends on the electromagnetic environment—oscillating charges emit light. The generated field can be expressed with the help of the dyadic Green’s tensor \mathbf{G} ,

$$\mathbf{E}_r(\mathbf{r}, \omega) = i\mu_0\omega \int_V d\mathbf{r}' \mathbf{G}(\mathbf{r}, \mathbf{r}', \omega) \cdot [-e\mathbf{j}(\mathbf{r}', \omega)],$$

which is the formal solution of Helmholtz’s equation [63],

$$\left[\nabla \times \frac{1}{\mu_r(\mathbf{r}\omega)} \nabla \times -\omega^2 \mu_0 \epsilon_0 \epsilon_r(\mathbf{r}\omega) \right] \mathbf{G}(\mathbf{r}, \mathbf{r}', \omega) = \delta(\mathbf{r}, \mathbf{r}'),$$

and characterizes the electromagnetic environment. The latter comprises foremost the boundary conditions of the field but can furthermore account for linear media ϵ_r, μ_r . This provides the flexibility to describe parts of the entire matter system in a simplified fashion while we focus our computational effort on the electronic structure considered via the paramagnetic current density \mathbf{j} . Such a separation becomes particularly interesting in multicomponent systems that extend over various length scales, e.g., molecule (described microscopically via \mathbf{j}) and solvent (described macroscopically via ϵ_r). This approach and its application to QED chemistry is detailed in Ref. [64]. As long as we treat the full system explicitly via the microscopic currents \mathbf{j} (as exemplified in the following), no limitation to the field

strength applies. The introduction of linear media on the other hand limits the evaluation to the linear response regime. The via \mathbf{G} embedded environment is obtained either analytically or numerically, a standard task for Maxwell solvers, and provides the realistic mode structure to which the electronic structure calculations couple. The energy associated with the radiated field should be taken correctly from the electronic system. Hence, the system of oscillating charges should feel a recoil force that accounts for any emitted energy—the radiation reaction, ensuring Newton’s third law. Consistent with the above bilinear coupling, the (dipolar) radiation-reaction potential $\hat{V}_{rr}(t) = -\hat{\mathbf{R}} \cdot \mathbf{E}_{r,\perp}(t) = -\hat{\mathbf{R}} \cdot \{ \mathcal{F}_t^{-1} [i\mu_0\omega \mathbf{G}_\perp(\omega)] * \int d\mathbf{r} [-e\mathbf{j}(\mathbf{r}t)] \}$, accounts now for the self-consistent interaction and the loss of energy due to photonic emission $\Delta E_{rr}(t) = \int_{t_0}^t dt' \dot{\hat{\mathbf{R}}}(t') \cdot \mathbf{E}_{r,\perp}(t')$. We notice that $\hat{V}_{rr}(t) \propto \hat{\mathbf{R}} \cdot \mathbf{G}_\perp \cdot \mathbf{j}$, i.e., the transverse projection of the paramagnetic current induces a (memory dependent) recoil acting back on the electronic system. In the case of free space, the radiation-reaction potential takes the form $\hat{V}_{rr}(t) = [-1/(6\pi\epsilon_0 c^3)] \times \partial_t^3 \hat{\mathbf{R}}(t) \cdot \hat{\mathbf{R}}$, which is consistent with the classical Abraham-Lorentz model [65,66] (more details in Supplemental Material II.D [62]). Calculating \mathbf{G} up front, the self-consistency is embedded solely via the current. This avoids the need to treat electronic structure and electromagnetic fields at the same time. The simplicity of the radiation-reaction potential represents the major strength of this approach, providing a swift and intuitive usage in a variety of electronic structure libraries.

Clearly, \mathbf{G} and any emerging parameters depend on the electromagnetic environment of our choice. Let us illustrate this conception in more detail for a strongly idealized one-dimensional waveguide ($\epsilon_r = \mu_r = 1$, with periodic boundaries in emission direction). The solution to the Helmholtz equation is then $\mathbf{G}_\perp(x, x', \omega) = \sum_{\mathbf{k}} \{ [S_{\mathbf{k}}(x) S_{\mathbf{k}}(x')] / [k^2 - (\omega/c)^2] \} \mathbf{e}_c \mathbf{e}_c^T$ with the eigemodes $S_{\mathbf{k}}(\mathbf{r}) = \sqrt{1/V} \times [\cos(kx) + \sin(kx)]$, $k = 2\pi n_x / L_x$, $n_x \in \mathbb{Z}$ and $\mathbf{e}_c \perp \mathbf{k}$. In combination with the inverse Fourier transformation and performing the long-wavelength approximation ($x = x' = 0$, details in Supplemental Material II.A [62]), the radiation-reaction potential takes the form $\hat{V}_{rr}(t) = \hat{\mathbf{R}} \cdot \mathbf{e}_c \sum_{\mathbf{k}} [1/(V\epsilon_0)] \int_{-\infty}^t dt' \cos[ck(t-t')] \int_V d\mathbf{r}' \mathbf{e}_c \cdot [-e\mathbf{j}(\mathbf{r}'t')]$. When the number of photonic modes is increased ($L_x \rightarrow \infty$), the dense mode structure will start to represent a photonic bath. Performing the explicit integration and employing the continuity equation for the integrated current $\int d\mathbf{r} [-e\mathbf{j}(\mathbf{r}t)] = \partial_t \hat{\mathbf{R}}(t)$, we obtain the radiation-reaction potential accounting for the recoil forces of emitting into the simplified waveguide $\hat{V}_{rr}^{1D}(t) = [(4\pi\hbar\alpha)/e^2] A^{-1} \mathbf{e}_c \cdot \dot{\hat{\mathbf{R}}}(t) \mathbf{e}_c \cdot \hat{\mathbf{R}}$. The coupling between the photonic continuum (representing the perfect wide-band limit) and the electronic system is provided by the fine-structure constant α divided by the cross-sectional area of the waveguide $A = V/L_x$.

The integrated emitted energy takes the form $\Delta E_{rr}(t) = [(4\pi\hbar\alpha)/e^2]A^{-1} \int_0^t dt' |\mathbf{e}_c \cdot \dot{\mathbf{R}}(t')|^2$.

While ångström thickness waveguides are possible [67], the majority of interesting systems (such as typical Fabry-Perot-type cavities) will feature comparably large quantization volumes, leading to a small influence of the radiation-reaction on the dynamics. Plasmonic systems represent here an exception due to their large currents and high mode-density at nanometer scales [68–70] which substantially enhances the emission of nearby molecular systems (Purcell-enhancement) as discussed later. An extended discussion and first generalizations to free-space and emission near mirrors can be found in the Supplemental Material, Secs. II. C and II. D [62]; we will remain here with our illustrative example.

TDDFT as example and self-consistent emission.— Time-dependent density-functional theory evolves around the concept that effective single-particle Kohn-Sham equations exist that are able to uniquely mimic all physical observables which are inherited by the original Coulomb Hamiltonian [43,44,71]. Our goal is now to provide a local potential that is as simple as possible to describe light-matter coupling and radiative emission consistent in the ordinary time-dependent Kohn-Sham equations $i\hbar\partial_t\phi_i(\mathbf{r}t) = \{-[\hbar^2/(2m_e)]\nabla^2 + v_s(\mathbf{r}t)\}\phi_i(\mathbf{r}t)$. The local Kohn-Sham potential $v_s = v_{\text{ext}} + v_{\text{Hxc}} + v_{rr}$ consists of the external potential v_{ext} (usually the nuclear binding potential), the electronic Hartree-exchange-correlation potential v_{Hxc} mimicking electronic many-body interactions, and the radiation-reaction potential v_{rr} accounts for the coupling to light. For each single-particle equation, the dipole-operator separates into single-coordinate contributions such that the radiation-reaction potential takes the trivial form

$$v_{rr}^{1D}(\mathbf{r}t) = \frac{4\pi\hbar\alpha}{e^2} A^{-1} \mathbf{e}_c \cdot \dot{\mathbf{R}}(t) \mathbf{e}_c \cdot (-e\mathbf{r}). \quad (1)$$

The potential can be added with virtually no effort to any TDDFT routine and accounts now consistently for excitation and radiative deexcitation according to Maxwell's equation of motion (see Supplemental Material II. B [62] for an alternative derivation from QEDFT). Figure 1 exemplifies the quick radiative decay of hydrogen driven by an external pulse (a) and the process of stimulated emission (b). Also strong-field effects such as high-harmonic generation can be described with the radiation-reaction potential (see Supplemental Material III [62]).

External perturbations δv_{appl} induce a response of the system which results in electronic motion and thus emission according to the radiation-reaction forces. In linear order, the response of the electronic density is given by $\delta\rho(\mathbf{r}t) = \int d\mathbf{r}' dt' \chi_s(\mathbf{r}, \mathbf{r}', t - t') [\delta v_{\text{appl}}(\mathbf{r}'t') + \int d\mathbf{r}'' dt'' f(\mathbf{r}', \mathbf{r}'', t' - t'') \delta\rho(\mathbf{r}''t'')]$. Here $f(\mathbf{r}', \mathbf{r}'', t' - t'') = \delta v_s(\mathbf{r}'t')/\delta\rho(\mathbf{r}''t'')$ is the kernel which accounts for the linear response of the Kohn-Sham potential (which depends

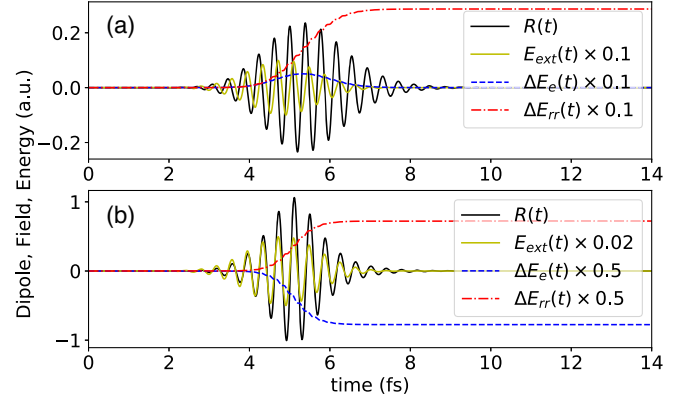


FIG. 1. Dipole $R(t)$ (black solid), relative electronic energy ΔE_e (blue dashed) and accumulated emitted radiation-reaction energy ΔE_{rr} (red dashed-dotted) for one-dimensional soft-coulomb hydrogen $v_{\text{ext}}(x) = e^2/(4\pi\epsilon_0\sqrt{x^2 + 1})$ emitting into a waveguide assuming a strongly Purcell-enhanced emission with $A^{-1} = 1/a_0^2$ for illustrative reasons. Notice that Purcell-enhancement factors of order $\Gamma/\Gamma_0 = \mathcal{O}(10^5)$ are not unusual. (a) An external laser-pulse $E_{\text{ext}}(t)$ (yellow, solid, amplified by a factor 10) drives the system out of its ground state. Energy deposited in the electronic system by the pulse is quickly radiated into the photonic bath. (b) Stimulated emission from the first excited electronic state under external driving. Details in the Supplemental Material IV [62].

self-consistently on the density) when the electronic density is perturbed. The contribution of the radiation-reaction forces $f_{rr}^{1D}(\mathbf{r}', \mathbf{r}'', \omega) = i4\pi\hbar\alpha A^{-1} \omega \mathbf{e}_c \cdot \mathbf{r}' \mathbf{e}_c \cdot \mathbf{r}''$ is explicitly memory dependent and thus frequency dependent, which allows it to provide a broadened resonance in contrast to the widely used frequency-independent adiabatic kernels that demand *ad hoc* broadening by hand. Assuming a single occupied (g) and a single unoccupied (e) Kohn-Sham orbital with bare excitation energy $\Omega_{eg} = \hbar\omega_{eg} = \epsilon_e - \epsilon_g$, the linear-response Casida equation can be solved analytically. We obtain the excitation poles $\Omega_n = \pm\Omega_{eg}[\sqrt{1 - (4\pi\alpha A^{-1}/e^2)^2 |\mathbf{e}_c \cdot \mathbf{R}_{eg}|^4} + i(4\pi\alpha A^{-1}/e^2) \times |\mathbf{e}_c \cdot \mathbf{R}_{eg}|^2]$ and the polarizability tensor, defined by $\mathbf{R}_{\text{induced}}(\omega) = \boldsymbol{\alpha}(\omega) \cdot \mathbf{E}_{\text{perturbation}}(\omega)$ [72], as

$$\begin{aligned} \Im\alpha_{\mu\nu}(\omega) &= \sum_{n=1}^{\infty} 2R_{gn}^{(\mu)} R_{ng}^{(\nu)} \frac{\Im\Omega_n}{(\hbar\omega - \Re\Omega_n)^2 + (\Im\Omega_n)^2} \\ &= 2R_{ge}^{(\mu)} R_{eg}^{(\nu)} \frac{\hbar\Gamma_{rr}}{(\hbar\omega - \Re\Omega_n)^2 + \hbar^2\Gamma_{rr}^2} \end{aligned}$$

with photoabsorption cross section and linewidth

$$\sigma(\omega) = \frac{4\pi\omega}{c} \Im\alpha(\omega), \quad \Gamma_{rr} = \frac{4\pi\alpha\omega_{eg}}{e^2} A^{-1} |\mathbf{e}_c \cdot \mathbf{R}_{eg}|^2.$$

A system has therefore no longer discrete excitations as common in TDDFT but features a physical linewidth Γ_{rr} .

In the perturbative limit, the latter is identical to the Wigner-Weisskopf solution $\Gamma_{WW}^{1D} = \omega_{eg} |\mathbf{e}_c \cdot \mathbf{R}_{eg}|^2 A^{-1} / \hbar \epsilon_0 c = \Gamma_{rr}$ (see also Supplemental Material IV. A [62]).

The radiative-reaction leads to a slight shift of the resonance as a consequence of the electromagnetic recoil $\propto 1 - (4\pi\alpha A^{-1}/e^2 |\mathbf{e}_c \cdot \mathbf{R}_{eg}|^2)/2$. This Lamb-shift effect indicates that the mass of the particle is changed, resulting in an adjusted physical mass of the electron. For Purcell-enhanced emission in a waveguide, the Lamb shift can take non-negligible values, especially when collective effects lead to collective Lamb-shift effects [73]. We obtain here for hydrogen ≈ 7 meV with $A^{-1} = 1/a_0^2$. However, for the vast majority of applications this shift is negligible and aspects such as the quality of the exchange-correlation potential in TDDFT are far more influential.

Let us point out that clearly also *ab initio* QED and QEDFT benefit from the radiation-reaction approach. Typically, only a few cavity modes play a substantial role in the strong coupling and the manifold of weakly interacting modes describe the emission profile, i.e., the loss channels, of the cavity. Using a radiation-reaction potential which represents a bath of free-space modes, cavity losses into free-space can be efficiently modeled as we will see in the following. Such a separation is of imminent importance for the future development of *ab initio* QED as it allows us to utilize higher level descriptions for a few most relevant cavity modes which explicitly account for the quantum features of light (see, e.g., [39]) while retaining the full manifold of modes that account on a simplified level for emission, linewidth, and loss. In this sense, the illustrated potential acts as a highly efficient realization of a bath, comparable to open-system strategies in quantum optics.

Electromagnetically induced transparency.—One excellent example of the strength of such a photonic-bath treatment is the description of electromagnetically induced transparency (EIT) [48,74]. Let us couple a single loss-free cavity mode, representing, for instance, a whispering-gallery mode, strongly to the hydrogen system. In addition, the matter system can emit light into a waveguide, i.e., a bath of photonic modes according to Eq. (1). Figure 2 presents how the absorption-profile of hydrogen changes with increasing strength of the bath and the coupling strength to the single mode. The interplay between the high-quality cavity mode and the lossy electromagnetic bath induces a window of transparency for strong radiative emission, i.e., the natural linewidth (black, dashed) obtains a sharp window of transparency (yellow, solid) at which the system can no longer absorb light. For increasing $g/\hbar\omega_c$, hydrogen and single mode begin to hybridize, resulting in the polaritonic states that characterize strong light-matter coupling. EIT has a plethora of technological applications, including effectively stopping or storing light [75,76], which become now for the first time available to TDDFT and QEDFT in a simple and intuitive way.

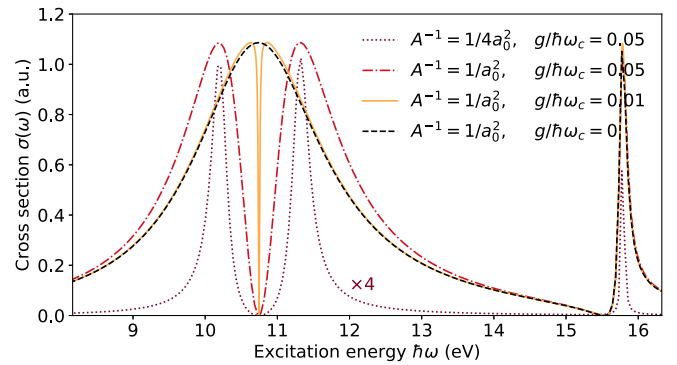


FIG. 2. Photoabsorption cross section $\sigma(\omega)$ of one-dimensional hydrogen coupled to a single cavity mode (strength $g = ea_0\sqrt{\hbar\omega_c/2\epsilon_0V}$) in resonance to $\Omega_{eg} = 10.746$ eV. With increasing strength of the photon bath A^{-1} , i.e., decreasing quality of the hydrogenic oscillator, the system moves from slightly broadened polaritonic resonances into the regime of electromagnetically induced transparency. Numerical details in the Supplemental Material IV [62].

While it is common practice to describe superradiant effects with quantum optical models [46] and the Purcell enhancement of spontaneous emission as perturbative correction to Wigner-Weisskopf theory [69], we show here that the radiation-reaction potential equips *ab initio* frameworks with the necessary tools to address those aspects self-consistently. In order to describe realistic systems, we implemented the radiative-reaction potential introduced in Eq. (1) in the TDDFT code GPAW [77] and use the computationally efficient LCAO basis [78] (see Ref. [79] for a tutorial).

Superradiant linewidth.—The synchronized evolution among a set of atoms or molecules amplifies their interaction with the photonic environment. Superradiance describes the effect that the synchronized emission is quicker than the individual emission [46]. For the single-photon absorption spectrum this takes the form of a linearly increasing linewidth with the size of the ensemble ($\Gamma \approx N_{Na_2}\Gamma_{Na_2}$) and is illustrated in Fig. 3 for a set of sodium dimers. The decisive strength of the *ab initio* implementation is the consistent treatment of radiative emission and matter, i.e., any form of Coulomb mediated interaction or charge migration is treated self-consistently. Figure 3 illustrates for instance a blueshift that originates from the Coulomb-mediated dipolar coupling between the individual dimers as observed in H aggregates [80]. Arranging the dimers in a head-to-tail orientation produces a redshift as typical for J aggregates (see Supplemental Material IV. C [62]). The radiation-reaction potential provides therefore consistently access to typical quantum optical and quantum chemical observables.

Plasmonic Purcell enhancement.—Plasmonic particles contribute in two ways to the quick decay of nearby molecules. First, strong dipolar oscillations of localized

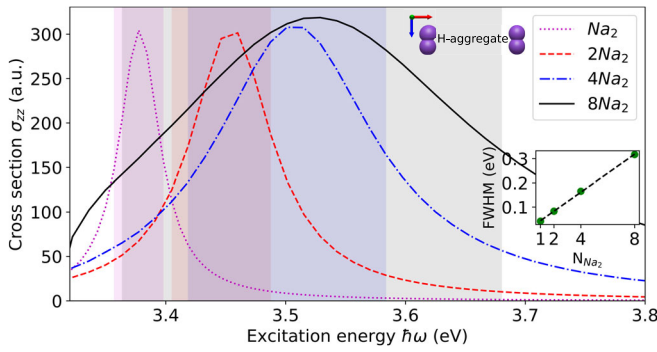


FIG. 3. Photoabsorption cross section $\sigma_{zz}(\omega)$ (zz component) for chains with variable length of far separated Na_2 . The dimer axis is oriented along z with a bond distance of 1.104 \AA , the chain along x has separations of 8 \AA (H-aggregate configuration). We used Eq. (1) with a quantization area of 35.05 \AA^2 and polarization along z . The emission rate or linewidth of the excitation around 3.5 eV increases linearly $\Gamma \approx N_{\text{Na}_2} \Gamma_{\text{Na}_2}$ with the length of the chain (see inset, $\text{FWHM} = 2\Gamma$ highlighted) as expected for the single-photon superradiant emission. The H-aggregate configuration is schematically illustrated. Numerical details in Supplemental Material IV. C [62].

surface plasmons result in quick radiative decay. Second and often dominant, they feature very quick internal dephasing on the fs timescale due to Landau damping and electron-electron scatterings. In combination with charge migration

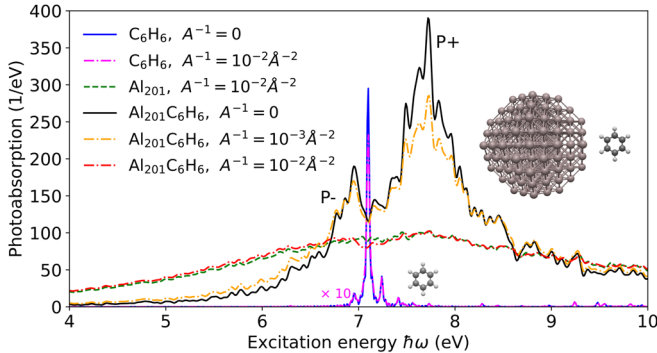


FIG. 4. Absorption spectrum in the x direction for isolated benzene (blue, magenta) and benzene strongly coupled to Al_{201} (black, red, yellow—upper and lower hybrid state P_{\pm} indicated). Dashed(-dotted) lines include emission via the radiation-reaction potential with polarization $\epsilon_c = \mathbf{e}_x$. The sharp excitation of benzene is only marginally broadened when including emission (magenta, dashed-dotted), i.e., atoms and molecules have comparably long lifetimes. Notice that the spectrum is slightly artificially broadened (details in Supplemental Material IV. D [62]). The sharp linewidth of benzene manifests in the fact that decreasing the cross-sectional area A leads to a minor broadening. The localized surface plasmon of the Al_{201} cluster radiates on the other hand substantially stronger (green, dashed). Coupled benzene inherits the short lifetime of the plasmon (red and yellow dashed-dotted)—any excitation is quickly transferred into the plasmon and either internally dephased or subsequently radiated into free-space. Numerical details in the Supplemental Material IV. D [62].

and hot-electron transfer between nanoparticle and molecule, this results in a complex dynamic which is theoretically challenging to capture. Full-fledged *ab initio* approaches provide here valuable results and following the radiation reaction, we can now easily and consistently account for radiative features that enrich quantum optical and electronic structure perspectives by a linking framework. Figure 4 illustrates the dipolar spectrum of benzene next to Al_{201} [18], including and excluding the radiative emission. The strong longitudinal fields around the plasmon lead to a hybridization of the bare plasmonic and $\pi - \pi^*$ benzene excitation, a purely Coulombic feature. For small cross-sectional surfaces $A = 10^2 \text{ \AA}^2$, the radiative contributions increase in relevance and strong plasmonic currents provide the previously slow radiating benzene excitation with an efficient emission channel—Purcell enhancement. The larger A the stronger internal dephasings compete with radiation, up to the point ($A^{-1} < 10^{-3} \text{ \AA}^{-2}$) where the Purcell enhancement for the emission of benzene is dominated by those internal losses. The competition between radiative and nonradiative decay channels is often tilted in favor of internal losses while nanoantenna design can invert this characteristic [81,82].

Conclusion.—Utilizing the dyadic Green’s tensor and deriving a subsequent local radiation-reaction potential, we illustrated how the electromagnetic fields can be easily embedded into electronic structure theory. This simple and computationally efficient ansatz allows to describe self-consistent light-matter interaction from first principles and is equivalent to solving Maxwell and Schrödinger equation hand in hand. The introduced radiation-reaction forces represent the recoil that ensures energy conservation during the emission of light. We demonstrated this ansatz for a simplified one-dimensional waveguide at the example of TDDFT, providing radiative emission, natural linewidths, strong coupling, electromagnetically induced transparency, Purcell enhancement and superradiant emission with virtually no additional computational effort. While we avoid the need to keep track of the electromagnetic fields, they are determined at any point in time by the dyadic Green’s tensor and the electronic currents, allowing a precise description of the experimentally measurable fields. Our ansatz is of generic use for any time-dependent electronic structure theory and can be extended to the nuclear degrees of freedom. In addition, we present generalizations to more complex electromagnetic environments in the Supplemental Material [62]. Implementing the radiation-reaction potential into the large-scale TDDFT code GPAW illustrates the high accessibility and seamless integration of our approach into existing *ab initio* libraries, paving the way for a stronger integration of light-matter and open-system features into the popular electronic structure approaches. A separation into microscopic \mathbf{j} and macroscopic components ϵ_r and the subsequent embedding of those macroscopic contributions into \hat{V}_{rr} paves a way to conveniently describe collective strong coupling at the

microscopic level. Collective strong coupling obtained recent interest in QED chemistry [83] and its application is detailed in Ref. [64].

We thank Jakub Fojt and Tuomas Rossi for assistance with GPAW as well as Michael Ruggenthaler and Ilya Tokatly for fruitful discussions. This work was supported by the Swedish Research Council (VR) through Grant No. 2016-06059 and the computational resources provided by the Swedish National Infrastructure for Computing (location Umeå) partially funded by the Swedish Research Council through Grant Agreement No. 2018-05973.

*christian.schaefer.physics@gmail.com

- [1] J. Li, H. U. Strand, P. Werner, and M. Eckstein, Theory of photoinduced ultrafast switching to a spin-orbital ordered hidden phase, *Nat. Commun.* **9**, 4581 (2018).
- [2] X. Li, T. Qiu, J. Zhang, E. Baldini, J. Lu, A. M. Rappe, and K. A. Nelson, Terahertz field-induced ferroelectricity in quantum paraelectric SrTiO₃, *Science* **364**, 1079 (2019).
- [3] D. Shin, S. Latini, C. Schafer, S. A. Sato, E. Baldini, U. De Giovannini, H. Hubener, and A. Rubio, Simulating terahertz field-induced transient ferroelectricity in quantum paraelectric SrTiO₃, [arXiv:2106.03957](https://arxiv.org/abs/2106.03957).
- [4] M. Sentef, M. Claassen, A. Kemper, B. Moritz, T. Oka, J. Freericks, and T. Devereaux, Theory of Floquet band formation and local pseudospin textures in pump-probe photoemission of graphene, *Nat. Commun.* **6**, 7047 (2015).
- [5] H. Hübener, M. A. Sentef, U. D. Giovannini, A. F. Kemper, and A. Rubio, Creating stable Floquet–Weyl semimetals by laser-driving of 3d dirac materials, *Nat. Commun.* **8**, 13940 (2017).
- [6] H. Hübener, U. De Giovannini, C. Schäfer, J. Andberger, M. Ruggenthaler, J. Faist, and A. Rubio, Engineering quantum materials with chiral optical cavities, *Nat. Mater.* **20**, 438 (2021).
- [7] N. Tancogne-Dejean, O. D. Mücke, F. X. Kärtner, and A. Rubio, Impact of the Electronic Band Structure in High-Harmonic Generation Spectra of Solids, *Phys. Rev. Lett.* **118**, 087403 (2017).
- [8] I. Floss, C. Lemell, G. Wachter, V. Smejkal, S. A. Sato, X.-M. Tong, K. Yabana, and J. Burgdörfer, *Ab initio* multiscale simulation of high-order harmonic generation in solids, *Phys. Rev. A* **97**, 011401(R) (2018).
- [9] E. Orgiu, J. George, J. A. Hutchison, E. Devaux, J. F. Dayen, B. Doudin, F. Stellacci, C. Genet, J. Schachenmayer, C. Genes, G. Pupillo, P. Samorì, and T. W. Ebbesen, Conductivity in organic semiconductors hybridized with the vacuum field, *Nat. Mater.* **14**, 1123 (2015).
- [10] J. Schachenmayer, C. Genes, E. Tignone, and G. Pupillo, Cavity-Enhanced Transport of Excitons, *Phys. Rev. Lett.* **114**, 196403 (2015).
- [11] X. Zhong, T. Chervy, S. Wang, J. George, A. Thomas, J. A. Hutchison, E. Devaux, C. Genet, and T. W. Ebbesen, Non-radiative energy transfer mediated by hybrid light-matter states, *Angew. Chem., Int. Ed. Engl.* **55**, 6202 (2016).
- [12] M. Du, L. A. Martínez-Martínez, R. F. Ribeiro, Z. Hu, V. M. Menon, and J. Yuen-Zhou, Theory for polariton-assisted remote energy transfer, *Chem. Sci.* **9**, 6659 (2018).
- [13] C. Schäfer, M. Ruggenthaler, H. Appel, and A. Rubio, Modification of excitation and charge transfer in cavity quantum-electrodynamical chemistry, *Proc. Natl. Acad. Sci. U.S.A.* **116**, 4883 (2019).
- [14] R. Sáez-Blázquez, J. Feist, A. I. Fernández-Domínguez, and F. J. García-Vidal, Organic polaritons enable local vibrations to drive long-range energy transfer, *Phys. Rev. B* **97**, 241407(R) (2018).
- [15] G. Groenhof, C. Climent, J. Feist, D. Morozov, and J. J. Toppari, Tracking polariton relaxation with multiscale molecular dynamics simulations, *J. Phys. Chem. Lett.* **10**, 5476 (2019).
- [16] A. F. Kockum, A. Miranowicz, S. De Liberato, S. Savasta, and F. Nori, Ultrastrong coupling between light and matter, *Nat. Rev. Phys.* **1**, 19 (2019).
- [17] D. Wang, H. Kelkar, D. Martín-Cano, T. Utikal, S. Götzinger, and V. Sandoghdar, Coherent Coupling of a Single Molecule to a Scanning Fabry-Perot Microcavity, *Phys. Rev. X* **7**, 021014 (2017).
- [18] T. P. Rossi, T. Shegai, P. Erhart, and T. J. Antosiewicz, Strong plasmon-molecule coupling at the nanoscale revealed by first-principles modeling, *Nat. Commun.* **10**, 3326 (2019).
- [19] J. A. Hutchison, T. Schwartz, C. Genet, E. Devaux, and T. W. Ebbesen, Modifying chemical landscapes by coupling to vacuum fields, *Angew. Chem., Int. Ed. Engl.* **51**, 1592 (2012).
- [20] A. Thomas, J. George, A. Shalabney, M. Dryzhakov, S. J. Varma, J. Moran, T. Chervy, X. Zhong, E. Devaux, C. Genet, J. A. Hutchison, and T. W. Ebbesen, Ground-state chemical reactivity under vibrational coupling to the vacuum electromagnetic field, *Angew. Chem., Int. Ed. Engl.* **55**, 11462 (2016).
- [21] F. Herrera and F. C. Spano, Cavity-Controlled Chemistry in Molecular Ensembles, *Phys. Rev. Lett.* **116**, 238301 (2016).
- [22] J. A. Campos-Gonzalez-Angulo, R. F. Ribeiro, and J. Yuen-Zhou, Resonant catalysis of thermally activated chemical reactions with vibrational polaritons, *Nat. Commun.* **10**, 4685 (2019).
- [23] C. Schäfer, J. Flick, E. Ronca, P. Narang, and A. Rubio, Shining light on the microscopic resonant mechanism responsible for cavity-mediated chemical reactivity, [arXiv:2104.12429](https://arxiv.org/abs/2104.12429).
- [24] X. Li, A. Mandal, and P. Huo, Cavity frequency-dependent theory for vibrational polariton chemistry, *Nat. Commun.* **12**, 1315 (2021).
- [25] T. E. Li, A. Nitzan, and J. E. Subotnik, Collective vibrational strong coupling effects on molecular vibrational relaxation and energy transfer: Numerical insights via cavity molecular dynamics simulations, *Angew. Chem., Int. Ed. Engl.* **60**, 15533 (2021).
- [26] S. Kühn, U. Håkanson, L. Rogobete, and V. Sandoghdar, Enhancement of Single-Molecule Fluorescence Using a Gold Nanoparticle as an Optical Nanoantenna, *Phys. Rev. Lett.* **97**, 017402 (2006).

- [27] N. J. Halas, S. Lal, W.-S. Chang, S. Link, and P. Nordlander, Plasmons in strongly coupled metallic nanostructures, *Chem. Rev.* **111**, 3913 (2011).
- [28] D. C. Marinica, M. Zapata, P. Nordlander, A. K. Kazansky, P. M. Echenique, J. Aizpurua, and A. G. Borisov, Active quantum plasmonics, *Sci. Adv.* **1**, e1501095 (2015).
- [29] R. Chikkaraddy, B. de Nijs, F. Benz, S. J. Barrow, O. A. Scherman, E. Rosta, A. Demetriadou, P. Fox, O. Hess, and J. J. Baumberg, Single-molecule strong coupling at room temperature in plasmonic nanocavities, *Nature (London)* **535**, 127 (2016).
- [30] J. Fregoni, G. Granucci, E. Coccia, M. Persico, and S. Corni, Manipulating azobenzene photoisomerization through strong light–molecule coupling, *Nat. Commun.* **9**, 4688 (2018).
- [31] B. Munkhbat, M. Wersäll, D. G. Baranov, T. J. Antosiewicz, and T. Shegai, Suppression of photo-oxidation of organic chromophores by strong coupling to plasmonic nanoantennas, *Sci. Adv.* **4**, eaas9552 (2018).
- [32] S. Franke, S. Hughes, M. K. Dezfouli, P. T. Kristensen, K. Busch, A. Knorr, and M. Richter, Quantization of Quasi-normal Modes for Open Cavities and Plasmonic Cavity Quantum Electrodynamics, *Phys. Rev. Lett.* **122**, 213901 (2019).
- [33] T. Neuman, D. S. Wang, and P. Narang, Nanomagnonic Cavities for Strong Spin-Magnon Coupling and Magnon-Mediated Spin-Spin Interactions, *Phys. Rev. Lett.* **125**, 247702 (2020).
- [34] J. Flick, H. Appel, M. Ruggenthaler, and A. Rubio, Cavity Born-Oppenheimer approximation for correlated electron-nuclear-photon systems, *J. Chem. Theory Comput.* **13**, 1616 (2017).
- [35] C. Schäfer, M. Ruggenthaler, and A. Rubio, *Ab initio* nonrelativistic quantum electrodynamics: Bridging quantum chemistry and quantum optics from weak to strong coupling, *Phys. Rev. A* **98**, 043801 (2018).
- [36] M. Ruggenthaler, N. Tancogne-Dejean, J. Flick, H. Appel, and A. Rubio, From a quantum-electrodynamical light-matter description to novel spectroscopies, *Nat. Rev. Chem.* **2**, 0118 (2018).
- [37] T. S. Haugland, E. Ronca, E. F. Kjønstad, A. Rubio, and H. Koch, Coupled Cluster Theory for Molecular Polaritons: Changing Ground and Excited States, *Phys. Rev. X* **10**, 041043 (2020).
- [38] T. S. Haugland, C. Schäfer, E. Ronca, A. Rubio, and H. Koch, Intermolecular interactions in optical cavities: An *ab initio* qed study, *J. Chem. Phys.* **154**, 094113 (2021).
- [39] C. Schäfer, F. Buchholz, M. Penz, M. Ruggenthaler, and A. Rubio, Making *ab initio* qed functional(s): Nonperturbative and photon-free effective frameworks for strong light-matter coupling, *Proc. Natl. Acad. Sci. U.S.A.* **118**, e2110464118 (2021).
- [40] M. Ruggenthaler, J. Flick, C. Pellegrini, H. Appel, I. V. Tokatly, and A. Rubio, Quantum-electrodynamical density-functional theory: Bridging quantum optics and electronic-structure theory, *Phys. Rev. A* **90**, 012508 (2014).
- [41] I. V. Tokatly, Time-Dependent Density Functional Theory for Many-Electron Systems Interacting with Cavity Photons, *Phys. Rev. Lett.* **110**, 233001 (2013).
- [42] J. Flick and P. Narang, Cavity-Correlated Electron-Nuclear Dynamics from First Principles, *Phys. Rev. Lett.* **121**, 113002 (2018).
- [43] E. Runge and E. K. U. Gross, Density-Functional Theory for Time-Dependent Systems, *Phys. Rev. Lett.* **52**, 997 (1984).
- [44] R. van Leeuwen, Mapping from Densities to Potentials in Time-Dependent Density-Functional Theory, *Phys. Rev. Lett.* **82**, 3863 (1999).
- [45] E. M. Purcell, Spontaneous emission probabilities at radio frequencies, in *Confined Electrons and Photons* (Springer, New York, 1995), p. 839.
- [46] M. Gross and S. Haroche, Superradiance: An essay on the theory of collective spontaneous emission, *Phys. Rep.* **93**, 301 (1982).
- [47] A. Goban, C.-L. Hung, J. D. Hood, S.-P. Yu, J. A. Muniz, O. Painter, and H. J. Kimble, Superradiance for Atoms Trapped Along a Photonic Crystal Waveguide, *Phys. Rev. Lett.* **115**, 063601 (2015).
- [48] M. Fleischhauer, A. Imamoglu, and J. P. Marangos, Electromagnetically induced transparency: Optics in coherent media, *Rev. Mod. Phys.* **77**, 633 (2005).
- [49] A. Rivas and S. F. Huelga, *Open Quantum Systems* (Springer, New York, 2012).
- [50] J. Yuen-Zhou, D. G. Tempel, C. A. Rodríguez-Rosario, and A. Aspuru-Guzik, Time-Dependent Density Functional Theory for Open Quantum Systems with Unitary Propagation, *Phys. Rev. Lett.* **104**, 043001 (2010).
- [51] K. Albrecht, A new class of schrödinger operators for quantized friction, *Phys. Lett.* **56B**, 127 (1975).
- [52] X. Zheng, F. Wang, C. Y. Yam, Y. Mo, and G. H. Chen, Time-dependent density-functional theory for open systems, *Phys. Rev. B* **75**, 195127 (2007).
- [53] R. Jestädt, M. Ruggenthaler, M. J. Oliveira, A. Rubio, and H. Appel, Light-matter interactions within the Ehrenfest–Maxwell–Pauli–Kohn–Sham framework: Fundamentals, implementation, and nano-optical applications, *Adv. Phys.* **68**, 225 (2019).
- [54] M. Noda, S. A. Sato, Y. Hirokawa, M. Uemoto, T. Takeuchi, S. Yamada, A. Yamada, Y. Shinohara, M. Yamaguchi, K. Iida *et al.*, Salmon: Scalable *ab-initio* light-matter simulator for optics and nanoscience, *Comput. Phys. Commun.* **235**, 356 (2019).
- [55] N. Tancogne-Dejean, M. J. Oliveira, X. Andrade, H. Appel, C. H. Borca, G. Le Breton, F. Buchholz, A. Castro, S. Corni, A. A. Correa *et al.*, Octopus, a computational framework for exploring light-driven phenomena and quantum dynamics in extended and finite systems, *J. Chem. Phys.* **152**, 124119 (2020).
- [56] N. M. Hoffmann, C. Schäfer, N. Säkkinen, A. Rubio, H. Appel, and A. Kelly, Benchmarking semiclassical and perturbative methods for real-time simulations of cavity-bound emission and interference, *J. Chem. Phys.* **151**, 244113 (2019).
- [57] C. M. Bustamante, E. D. Gadea, A. Horsfield, T. N. Todorov, M. C. González Lebrero, and D. A. Scherlis, Dissipative Equation of Motion for Electromagnetic Radiation in Quantum Dynamics, *Phys. Rev. Lett.* **126**, 087401 (2021).

- [58] J. Flick, D. M. Welakuh, M. Ruggenthaler, H. Appel, and A. Rubio, Light–matter response in nonrelativistic quantum electrodynamics, *ACS Photonics* **6**, 2757 (2019).
- [59] K. M. Birnbaum, A. Boca, R. Miller, A. D. Boozer, T. E. Northup, and H. J. Kimble, Photon blockade in an optical cavity with one trapped atom, *Nature (London)* **436**, 87 (2005).
- [60] E. A. Power and S. Zienau, Coulomb gauge in non-relativistic quantum electro-dynamics and the shape of spectral lines, *Phil. Trans. R. Soc. A* **251**, 427 (1959).
- [61] C. Schäfer, M. Ruggenthaler, V. Rokaj, and A. Rubio, Relevance of the quadratic diamagnetic and self-polarization terms in cavity quantum electrodynamics, *ACS Photonics* **7**, 975 (2020).
- [62] See Supplemental Material at <http://link.aps.org/supplemental/10.1103/PhysRevLett.128.156402> for numerical details, an introduction into QED, a generalized discussion of the radiation-reaction ansatz, a detailed derivation of the radiation-reaction potential for various environments, a comparison to QEDFT and the Abraham-Lorentz model, applications to extended systems and high-harmonic generation.
- [63] S. Y. Buhmann, *Dispersion Forces I: Macroscopic Quantum Electrodynamics and Ground-State Casimir, Casimir-Polder and van der Waals Forces* (Springer, New York, 2013), Vol. 247.
- [64] C. Schäfer, Dynamic of Single Molecules in Collective Light-Matter States from First Principles, [arXiv:2204.01602](https://arxiv.org/abs/2204.01602).
- [65] J. A. Wheeler and R. P. Feynman, Interaction with the absorber as the mechanism of radiation, *Rev. Mod. Phys.* **17**, 157 (1945).
- [66] J. D. Jackson, *Classical Electrodynamics* (John Wiley & Sons, New York, 1999).
- [67] X. Zhang, C. De-Eknamkul, J. Gu, A. L. Boehmke, V. M. Menon, J. Khurgin, and E. Cubukcu, Guiding of visible photons at the ångström thickness limit, *Nat. Nanotechnol.* **14**, 844 (2019).
- [68] E. Ozbay, Plasmonics: Merging photonics and electronics at nanoscale dimensions, *Science* **311**, 189 (2006).
- [69] A. F. Koenderink, On the use of purcell factors for plasmon antennas, *Opt. Lett.* **35**, 4208 (2010).
- [70] M. P. Nielsen, X. Shi, P. Dichtl, S. A. Maier, and R. F. Oulton, Giant nonlinear response at a plasmonic nanofocus drives efficient four-wave mixing, *Science* **358**, 1179 (2017).
- [71] E. Engel and R. M. Dreizler, *Density Functional Theory* (Springer, New York, 2013).
- [72] C. A. Ullrich, *Time-Dependent Density-Functional Theory: Concepts and Applications* (Oxford University Press, Oxford, 2011).
- [73] R. Röhlberger, K. Schlage, B. Sahoo, S. Couet, and R. Ruffer, Collective lamb shift in single-photon super-radiance, *Science* **328**, 1248 (2010).
- [74] B. Peng, Ş. K. Özdemir, W. Chen, F. Nori, and L. Yang, What is and what is not electromagnetically induced transparency in whispering-gallery microcavities, *Nat. Commun.* **5**, 5082 (2014).
- [75] L. V. Hau, S. E. Harris, Z. Dutton, and C. H. Behroozi, Light speed reduction to 17 metres per second in an ultracold atomic gas, *Nature (London)* **397**, 594 (1999).
- [76] C. Liu, Z. Dutton, C. H. Behroozi, and L. V. Hau, Observation of coherent optical information storage in an atomic medium using halted light pulses, *Nature (London)* **409**, 490 (2001).
- [77] J. Enkovaara, C. Rostgaard, J. J. Mortensen, J. Chen, M. Dułak, L. Ferrighi, J. Gavnholt, C. Glinsvad, V. Haikola, H. Hansen *et al.*, Electronic structure calculations with GPAW: A real-space implementation of the projector augmented-wave method, *J. Phys. Condens. Matter* **22**, 253202 (2010).
- [78] M. Kuisma, A. Sakko, T. P. Rossi, A. H. Larsen, J. Enkovaara, L. Lehtovaara, and T. T. Rantala, Localized surface plasmon resonance in silver nanoparticles: Atomistic first-principles time-dependent density-functional theory calculations, *Phys. Rev. B* **91**, 115431 (2015).
- [79] GPAW tutorial to the radiation-reaction potential, https://wiki.fysik.dtu.dk/gpaw/tutorialsexercises/opticalresponse/radiation_reaction/rtddft.html (accessed: 2022-01-17).
- [80] M. Kasha, H. Rawls, and M. A. El-Bayoumi, The exciton model in molecular spectroscopy, *Pure Appl. Chem.* **11**, 371 (1965).
- [81] L. Rogobete, F. Kaminski, M. Agio, and V. Sandoghdar, Design of plasmonic nanoantennae for enhancing spontaneous emission, *Opt. Lett.* **32**, 1623 (2007).
- [82] J. J. Baumberg, J. Aizpurua, M. H. Mikkelsen, and D. R. Smith, Extreme nanophotonics from ultrathin metallic gaps, *Nat. Mater.* **18**, 668 (2019).
- [83] T. W. Ebbesen, Hybrid light–matter states in a molecular and material science perspective, *Acc. Chem. Res.* **49**, 2403 (2016).